8-9-2022

Ex vivo biomechanical comparison of a novel compression screw fastener and traditional AO cortical bone screw for fixation of a simulated slab fracture in the equine third carpal bone

Allison Salinger
asaling@vt.edu

Ex vivo biomechanical comparison of a novel compression screw fastener and traditional AO cortical bone screw for fixation of a simulated slab fracture in the equine third carpal bone

By

Allison Salinger

Approved by:

Cathleen A. Mochal-King (Major Professor)
Lauren B. Priddy
Michael Jaffe
Larry Hanson (Graduate Coordinator)
Kent H. Hoblet (Dean, College of Veterinary Medicine)

A Thesis
Submitted to the Faculty of
Mississippi State University
in Partial Fulfillment of the Requirements
for the Degree of Master of Science
in Veterinary Science
in the Department of Pathobiology and Population Medicine

Mississippi State, Mississippi

August 2022

Name: Allison Salinger

Date of Degree: August 9, 2022

Institution: Mississippi State University

Major Field: Veterinary Science

Major Professor: Cathleen A. Mochal-King

Title of Study: Ex vivo biomechanical comparison of a novel compression screw fastener and traditional AO cortical bone screw for fixation of a simulated slab fracture in the equine third carpal bone

Pages in Study 37

Candidate for Degree of Master of Science

Frontal plane slab fractures account for the majority of third carpal bone (C3) fractures in performance horses. Treatment is stabilization with an AO cortical screw. Complications are fragment splitting, fragment spinning, and irritation of dorsal soft tissue structures. A novel, headless, cannulated screw with interlocking threads (the Headless Compression Screw Fastener, HCSF) has been developed to resist multidirectional forces. Simulated C3 slab fractures were created in nine paired equine carpi. HCSF or AO cortical screws were loaded in shear to failure. Stiffness, maximum load to failure, and yield load was assessed in linear mixed models. No significant difference was detected in maximum load to failure, stiffness, or yield load. Mode of failure was screw bending in all specimens. The HCSF successfully repaired simulated third carpal bone fractures. The design eliminates counter sinking. There was no significant difference compared to the cortical screws. These results promote clinical application.

ACKNOWLEDGEMENTS

The author expresses her sincere gratitude to OsteoCentric Technologies for providing the Headless Compression System for use in this study. Mechanical testing would not be possible without Dr. Lauren Priddy and Dr. Steven Elder- their bioengineering expertise was invaluable for this project. Specimen storage, collection, and methodology would not be possible without Dr. Ben Nabors. Thank you to Kailey Clinton for her contributions to data acquisition, data interpretation, creation of figures, and methodology. Sincere gratitude must be given to my major professor Dr. Mochal and to Dr. Jaffe for sharing their knowledge of orthopedic surgery. Additionally, I would thank all the staff at Mississippi State University for making this manuscript possible.

TABLE OF CONTENTS

LIST OF TABLES

LIST OF FIGURES

CHAPTER I

INTRODUCTION

Musculoskeletal injuries in racehorses can have profound negative impacts on animal well-being, training programs, and financial stakeholders. Carpal fractures frequently occur in racehorse breeds, including Thoroughbreds, Standardbreds, and American Quarter Horses.[1-6] High speed exercise imposes repetitive impact loading on the dorsal aspect of the third carpal bone (C3), causing remodeling and sclerosis of the radial fossa.[7] Frontal plane C3 slab fractures of the radial facet are the most common carpal bone fracture type as a result of shear forces.[4,7,8]

Conservative treatment of C3 slab fractures results in severe osteoarthritis, ending the performance career of the animal. Thus, fragment removal or stabilization is imperative, regardless of the horse's intended level of activity following recovery. Fragments less than 10-mm may be removed, although preservation and stabilization of the articular surface is preferred.[9] Interfragmentary stabilization is typically achieved by placing one cortical screw using lag technique across the slab fracture.[9,10]

Intra-operative complications associated with C3 fracture repairs include fragment spinning or fragmentation during screw tightening.[11] Additionally, failure to obtain an ideal countersink can cause displacement of fragments when working with a thin cortex. Fragments less than 10-mm thick are at an increased risk of fragmentation during countersinking. However, failure to countersink can result in dorsal soft tissue irritation and fibrosis. Although results vary among studies, return to racing has been reported to be as low as 42% in Thoroughbreds after C3

slab fracture fixation.[5] Investigation of new implants is therefore warranted in an effort to decrease the incidence of complications, preserve the articular surface, and ultimately produce better outcomes.

Cortical screws are designed for use in hard cortical bone and are heavily utilized in equine orthopedic surgery. Traditional cortical screws contain a buttress thread, which is limited to resisting only a unidirectional force.[12,13] Recently, a novel Bone-Screw-Fastener has been integrated into human orthopedic surgery.[12-14] The screw-fastener has an interlocking thread pattern capable of resisting multidirectional forces and a reverse cutting flute mechanism which prevents iatrogenic bone destruction.[12,13] A cadaveric mechanical study has demonstrated superior protection from torque stripping forces of this new screw when compared to the buttress screw in human tibiae.[12]

Similar to the Bone-Screw-Fastener, the Headless Compression Screw Fastener (HCSF) has interlocking thread technology which improves the direct connection of osseous tissue to the implant.[15] This osseointegration leads to a functional, congruous relationship between the bone and screw.[16] The HCSF achieves compression as it is advanced, and unlike the Bone-Screw-Fastener, has the added benefit of a headless design. This design eliminates the need to countersink, and taken collectively with its interlocking nature, may decreases the risk of fragmentation, displacement, and articular interference. Problems associated with creating a shallow countersink or not countersinking may potentially be avoided when using the HCSF in place of a cortical bone screw.

There are no known published applications of the HCSF in equine veterinary medicine to the authors' knowledge. The objective of this study to was to compare the maximal singular shear force to failure, stiffness, and yield load created by a mechanical testing device of a 3.9-

mm HCSF to a 3.5-mm standard AO cortical bone screw. We hypothesized that the 3.9-mm HCSF would have superior mechanical shear performance compared to the 3.5-mm standard cortical bone screw when applied in lag screw fashion for fixation of a simulated C3 frontal plane slab fracture in cadaveric equine third carpal bones.

CHAPTER II

FATIGUE AND FRACTURE OF THE EQUINE CARPUS

Anatomy

The equine carpus is a hinge joint consisting of 2 rows of cuboidal bones. The proximal surface of the proximal row of carpal bones articulates with the radius (antebrachiocarpal joint). This row of cuboidal bones consists of the radial carpal bone, intermediate carpal bone, ulnar carpal bone, and accessory carpal bones. The proximal surface of the distal row of carpal bones articulates with the proximal row of carpal bones (middle carpal joint- Figure 1). The distal surface of the distal row of carpal bones communicates with the metacarpal bones (carpometacarpal joint). This row of cuboidal bones consists of the second, third, and fourth carpal bones. The C3 is the largest of the 3 distal row bones. It has an irregular shape, with a palmar and dorsal portion. The dorsal portion contains the radial and intermediate facets which are divided by a prominently raised sagittal ridge.[17] Cuboidal bones such as the C3 are covered in articular cartilage, under which is a shell of cortical bone. The cortical bone houses the inner trabecular bone.

These cuboidal bones are architecturally complex and allow for various ranges of motion and joint compartment communications with their associated soft tissue structures and joint capsule arrangements. The middle carpal and carpometacarpal joints always communicate with one another. Although the antebrachiocarpal and middle carpal joints have not proven to communicate in a previous imaging study, one investigation demonstrated mepivacaine diffusion

between the two joint spaces in > 80% of limbs tested.[18,19] These joints vary greatly in their degree of flexion, with the antebrachiocarpal joint allowing for a great degree of flexion, the middle carpal joint allowing for a moderate degree of flexion, and the carpometamarpal joint allowing for very minimal flexion. Interosseous ligaments and the palmar carpal ligament maintain carpal alignment and prevent hyperextension, however, overextension is not always preventable at high speeds.[17]

Anatomy in Motion

During fast paced work, the metacarpus becomes dorsally displaced relative to the radius.[20] This exacerbates the shear force exerted on the C3, particularly the radial facet, as the radiocarpal bone articulates solely with the radial facet when the joint is hyperextended.[21] Repetitive forces lead to fatigue, a process by which microscopic damage accumulates, sometimes until complete failure (i.e. fracture) occurs.[22,23] In the C3, subchondral damage will often precede the development of lameness and slab fractures, however subchondral lesions are not always seen radiographically.[24-26] Association with high speed work, the fracture arising in a consistent location, and the fracture coursing through the bone in predictable course are all met criteria for inclusion as a stress or fatigue related fracture.[27] As with most racehorse fractures, C3 slab fractures result from the accumulation of microdamage that is not allowed adequate time to remodel, ultimately weakening the bone and predisposing it to fracture.

Wolfe's Law

Remodeling is a process by which abnormal bone is resorbed by osteoclasts and replaced by osteoblasts at the same location. This is a manifestation of Wolfe's law, which theorizes that bone is a dynamic organ which adapts to mechanical stress. Simply put, bone is removed where

it is not needed and laid down where it is needed.[28-35] It is the lag time in between bone resorption and bone formation that increases the structural vulnerability of the bone.[36] Histomorphometrical findings as these structural properties are weakened include both trabecular microfractures and trabecular increases in bone mineral density, suggesting that marked metabolic activity is occurring in an attempt to strengthen the bone.[36] Trabecular widening (microcracks) and increased porosity (a result of the resorptive phase of remodeling) are intimately associated with shear stress.[27,37]

Biomechanical Forces

Shear stress occurs when forces are applied parallel to a surface. When forces act on an object, the object will deform to some degree. The ability of an object to deform and return to its original shape once the load has been removed is illustrated in the elastic region of a load deformation curve. Stiffness is defined as the slope of the elastic portion of the curve. Once the object is no longer able to return to its original shape, a yield point is reached and permanent deformation occurs. The plastic region of the load deformation curve is that to the right of the yield point. Plastic deformation is the phase which leads to failure. The load deformation curve portrays information about the structural (dimensional) properties of bone.[38,39]

Stress (σ) is defined as the force divided by the area of the object that it acts upon. Normal stress occurs when forces are applied perpendicular to the surface of a structure as opposed to shear stress (forces applied parallel to the surface). Strain (ε) refers to the change in dimension of the object divided by the original dimension, often expressed as a percentage. By calculating the stress and strain, information about the mechanical (material) properties of bone can be elucidated, eliminating geometrical influence. When stress is considered normal, the slope of the curve is referred to as Young's modulus. When shear stress predominates, the slope is

referred to as shear modulus. Yield and failure points are conceptually similar to that described for load deformation curves.[38,39]

Mechanical properties of bone are dependent on the direction of the forces applied. Cortical bone is anisotropic due to protein fiber arrangements, osteon composition, and mineral composition. Trabecular bone is anisotropic because of fiber arrangements, osteon composition, mineral composition, and porosity. Porosity is a unique characteristic of trabecular bone that allows it to store more energy prior to failure, compared to cortical bone. Despite the C3 being composed of mostly trabecular bone, fractures can still occur if adaptive healing cannot keep pace with lytic processes.[38,40]

Fracture Healing

Once a fracture occurs, healing can ensue by means of indirect or direct healing. If healing is abnormal, bones are subject to delayed unions, nonunions, or malunions. Callous formation, instability, and incongruency of articular surfaces of the C3 can lead to osteoarthritis of the equine carpus. For this reason, precise reduction of C3 slab fractures should be attempted surgically.

Contact healing is the most ideal form of fracture healing, however, such rigid fixation is often not possible. Fracture gaps smaller than 0.01 mm allow for direct contact healing, and subsequently form little or no callous and no interfragmentary motion.[41] If contact healing can occur, cutting cones form adjacent to osteons at the fracture site.[42] Osteoclasts remove bone at the end of the cutting cone, while trailing osteoblasts will lay down new bone. Osteons remodel into lamellar bone. This efficient process allows for direct re-establishment of the bony architecture without production of a callous.

Gap Healing is the second type of direct healing that can only occur if the fracture gap is less than 1 mm.[41] Before the reconstructive phase (similar to contact healing) can occur, lamellar bone fills the fracture gap perpendicular to the long axis.[43] This mechanically weak scaffold contains osteoprogenitor cells which produce osteoblasts. Not until the lamellar bone is fully constructed can the remodeling process begin.[44]

When interfragmentary compression and fracture stability are less ideal, indirect healing takes place. This process is broken down into several steps: the inflammatory phase, endochondral formation, intramembranous formation, repair, and remodeling. The hallmark of the acute inflammatory phase is hematoma formation at the fracture site. Hematoma formation is immediate and proinflammatory mediators predominate over the course of about 7 days.[45] Granulation tissue will eventually form within the hematoma, and endochondral formation commences. A cartilaginous, "soft callous" develops about 7-9 days post trauma, extraperiostally. Subperiostally, intramembranous ossification begins, forming the "hard callous." Angiogenesis, mineralization, and resorption of the cartilaginous callous precede the remodeling phase. Hard callous formation is typically complete by day 14, which involves calcified cartilage being replaced by woven bone and can be referred to as the repair phase.[46] Remodeling may occur around 3-4 weeks after the traumatic event.[47] During the remodeling phase, woven bone is replaced with lamellar bone. Lamellar bone is more mature and stronger than its precursor, woven bone. Many factors influence bone healing time, however indirect healing undoubtfully takes longer than direct healing.

As stated previously, the equine C3 is trabecular bone covered with a thin cortical shell. Fractures of trabecular or cancellous bone heal differently than cortical bone. Periosteal callous formation does not typically form unless there is much instability. Intramembranous ossification

causes bridging of new bone between trabeculae before union of the cortical shell.[48] Still, well aligned and stable lag screw fixation is crucial to maintain the health of the joint.

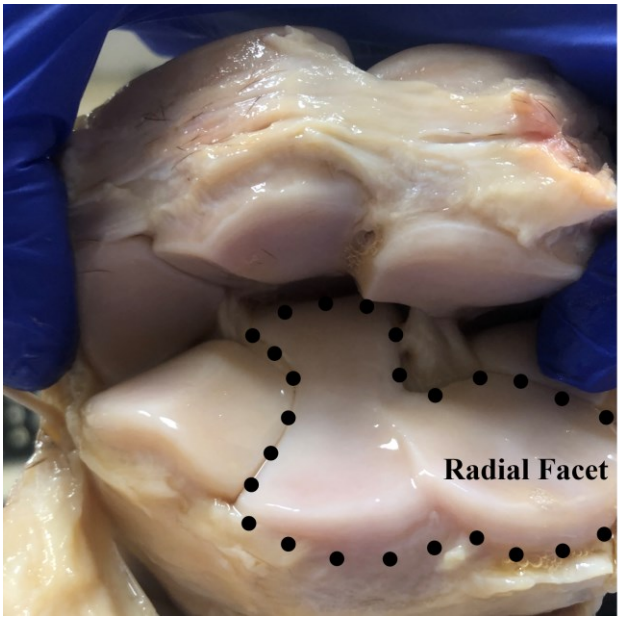

Figure 1 Middle carpal joint

Right middle carpal joint. The C3 is outlined with the dotted line. Medial is to the right, lateral is to the left.
Credit: Salinger personal photograph

CHAPTER III

HISTORY AND FUTURE OF THE SCREW

One of the earliest and most famous accounts of the screw dates back to third century BCE. Archimedes (287-212 BC) is considered by many to have invented the water screw during this time period.[49] The water screw was in fact a water conveyer, consisting of a large wooden screw inside of a tubular structure that transported low-lying water to higher ground for irrigation.[50] One end of the water screw would be submerged in water, while the other end would be elevated above the ground surface. As the helix was cranked by hand, water was lifted and transported above the ground surface.

The water screw was a simple machine that converted rotational motion of water into linear motion of water. Current day screws used in countless industries follow the same principle, except that the screw is engaged in a solid material and is advanced forward itself as it is rotated. Craftsmen began producing screws as early as the 18th century, while surgeons began utilizing screws in the 19th century.[50] Alloys have varied throughout the years, with wood/ steel and nickel-plated screws being used in orthopedic surgery in the 19th century and vanadium machine screws being advocated for in the early 20th century.[51,52] In 1958 a group of Swiss surgeons developed the Arbeitsgemeinschaft für Osteosynthesefragen (AO). Through research, innovation, clinical documentation, development of orthopedic implants and instruments, as well as providing international educational opportunities, this group has revolutionized both human and veterinary orthopedic surgery.[53]

Great improvements and advancements in orthopedic surgery have been met since the advent of the AO, however, stainless steel, buttress threaded screws have been the conventional screw since Robert Danis invented the design in the 1940's.[13] As described by Stahel et al., shortcomings of the buttress screw are as follows:

1. The screws can be hard to start within the bone interface.
2. The screws can miss the far cortex through the projected trajectory, leading to near cortex stripping.
3. Near and far cortex stripping can occur if too much torque is applied.
4. Threads induce a radial force perpendicular to the screw's long axis, which can act as a stress riser or increase chances of incidental fracturing.
5. The buttress design can resist only unidirectional loads.
6. Screw loosening and "toggling" may occur if the screw hole enlarges, leading to failure.
7. A rough, imprecise cutting mechanism in which debris accumulates along the thread teeth can lead to both microfractures and heat generation.

A limitation perhaps specifically applying to C3 fracture repair is one argument that buttress threads are unable to develop sufficient insertion torque in trabecular or osteopenic bone to provide enough compression to resist shear forces.[14] Bone-screw-fasteners have been designed with interlocking threads to generate compression, prevent stripping, and resist multidirectional loads (Figure 2).[12-14] Higher torque stripping resistance was verified in a human cadaveric study.[12] Recently, the effect of interlocking screws used for cadaveric canine humeral condylar fracture repair was investigated by Raleigh, et al. Interlocking screws were found to have significantly (18.5- 23.2%) greater loads to failure compared to buttress screws.[54] With such

promising results, the influence of the interlocking screw for use in C3 frontal plane slab fractures became of interest and inspired composition of the current study.

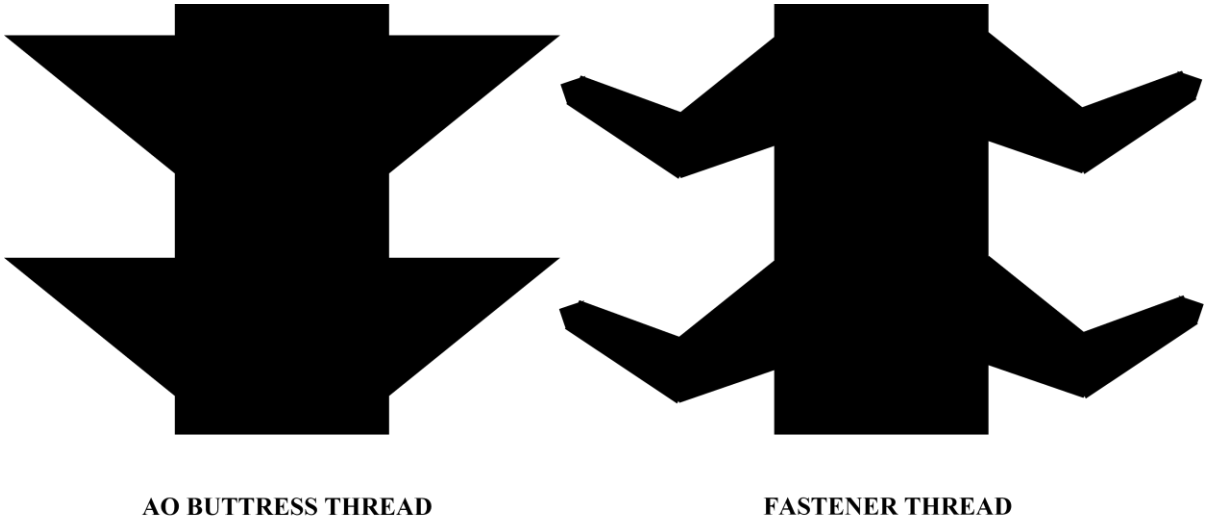

Figure 2 Traditional AO buttress thread screw versus interlocking bone-screw-fastener. Credit: Schematic created by Salinger, simplified figure from *Alfonso, et al.*

CHAPTER IV

MATERIALS AND METHODS

Specimens

Eighteen paired forelimbs collected from 9 horses were used for this ex vivo study (3 to 20 years of age, 5 geldings, 1 stallion, and 3 mares). Breeds included six American Quarter Horses, one Warmblood, and two grade type horses. Weights ranged from 314- 595 kg. Horses were euthanized for reasons unrelated to the project and were without clinical, gross, and radiographic carpal abnormalities. Forelimbs were transected mid-radius within 24 hours following euthanasia. The specimens were wrapped in towels soaked in a 0.9% sodium chloride solution, secured in a plastic bag, and stored at -25°C for up to 3 months. The forelimbs were thawed in a 0.9% sodium chloride solution at room temperature 24 hours prior to testing. For each pair, the left or right carpi was randomly assigned to receive fixation with either a HCSF or a cortical screw. Once thawed, the limbs were dissected, and the distal row of carpal bones were isolated from the specimens.

Preparation

A 10-mm wide simulated C3 frontal plane slab fracture of the radial facet was created with a hand saw. The distal row of carpal bones was first secured in a vice, and a template-guided osteotomy was made across the radial facet of the third carpal bone. The fragment was reduced and secured with a Verbrugge Bone Holding Forcep (Sontec Instruments, Centennial, CO) prior to screw placement.

For specimens repaired with cortical screws, fragments were reduced with one 3.5-mm diameter, 40-mm long, self-tapping 316 stainless steel AO cortical bone screw (Figure 3) in lag fashion. The screw was aligned in the center of the fragment, perpendicular to the frontal fracture plane using standard AO/ASIF technique. A 3.5-mm glide hole and 2.5-mm thread hole were drilled through the palmar aspect of the cis cortex to ensure adequate depth for the standardized 40-mm long screws. Radiographs were taken after placement to ensure adequate fragment compression (Figure 6a).

For specimens repaired with the HCSF, fragments were reduced with one 3.9-mm diameter, 40-mm long, cannulated, self-tapping, ASTM F136 Titanium HCSF screw (Figure 3). A 3.5 mm drill bit (DePuy Synthes, West Chester, PA) was aligned as described for the cortical screw group and drilled across the fragment through the cis cortex. Due to their self-compressing nature, HCSF screws do not require a glide hole to be drilled. The screws were advanced into the bone with a 2.0-mm hexagonal-head cannulated screw driver (OsteoCentric Technologies, Logan, UT) until they were flush with the dorsal surface of C3. Adequate reduction was verified with radiographs (Figure 6b).

Biomechanical Testing

The distal row of carpal bones was mounted into a custom-made steel rectangular pot using polyurethane casting resin (Specialty Resin & Chemical, Kalamazoo, MI), such that the osteotomy site was protruding from the pot. The resin was allowed 10 minutes to cure to ensure the parent bone was secured within the construct. The osteotomy site was aligned perpendicularly to the platform and monitored as the polyurethane cured to ensure that the resin did not adhere to the osteotomy site or the fragment. The potted bone was fitted to a universal testing machine (MTI-2K, Measurements Technology, Inc., Marietta, GA), equipped with a

2,000-lbf load cell (Figure 4). The custom platen block was aligned with the proximal surface of the dorsal bone fragment and was translated downwards to apply shear force to the specimen. Specimens were tested in shear in a single cycle to failure under a displacement control at a rate of 100 mm/min.

Data Analyses

For each mechanical test, a load-deformation curve was produced (Figure 5). Maximum load to failure (N), stiffness (N/mm), and yield load (N) were analyzed for each specimen. Maximum load to failure was defined as the maximum force applied during testing. Stiffness was defined as the slope of the elastic (linear) portion of the load-deformation curve. For samples that had plastic deformation prior to failure, yield load was defined using an offset method of 1 mm displacement.[55-57] Yield load was defined as the maximum load in samples without plastic deformation prior to failure.

Statistical Analyses

The effect of screw type on maximum load to failure, stiffness, and yield load was assessed in separate linear mixed models using the mixed procedure in SAS for Windows v9.4 (SAS Institute, Inc., Cary, NC). Screw, side of limb, and their interaction were the initial fixed effects while horse identity was included as a random effect. If the interaction term was not significant, it was removed from the model and a main effects only model was tested. In turn, if side of limb was not significant, it was removed from the model. Visual assessment of the conditional residuals was done to ensure the assumptions of normality and homoscedasticity had been met. An alpha level of 0.05 was used to determine significance.

Figure 3 3.5 mm AO cortical screw versus 3.9 mm Headless Compression Screw Fastener

Cortical screw is on the left. Headless Compression Screw Fastener is on the right.
Credit: Salinger personal photograph

Figure 4 A repaired simulated C3 slab fracture secured in the testing machine.

The osteotomy is parallel to the axis of loading. The arrow demonstrates the direction of the platen block as it moves towards the dorsal surface of the fragment, allowing it to be tested in shear.
Credit: Salinger personal photograph

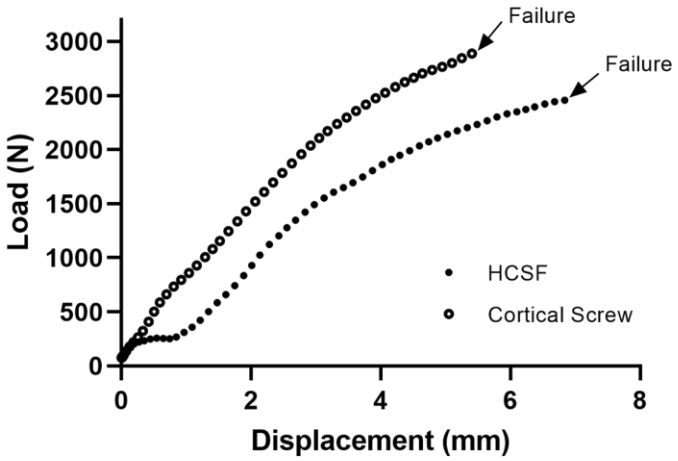

Figure 5 Representative load displacement curve

Representative load displacement curve for specimen tested in the HCSF and Cortical Screw groups, single cycle to failure shear test. The failure point is recorded as the highest load value attained.
Credit: Graph created by Kailey Clinton

CHAPTER V

RESULTS

Fragment reduction was considered acceptable for all specimens as no osteotomy gap was observed radiographically (Figure 6a and Figure 6b). For HCSF repaired specimens, average maximum load to failure was 2305.54 +/- 633.44 N, average stiffness was 382.89 +/- 95.27 N/mm, and average yield load was 2291.97 +/- 642.11 N. Specimens repaired with cortical screws had an average maximum load to failure of 2930.19 +/- 707.43 N, an average stiffness of 427.59 +/- 128.52 N/mm, and an average yield load of 2896.58 +/- 678.57 N (Table 1).

No effect of screw type was detected in terms of maximum load to failure ($p= 0.084$), stiffness ($p= 0.26$), or yield load ($p= 0.088$). Mode of failure was screw bending in all specimens (Figure 6c and Figure 6d). Three cortical screws and four HCSF screws exhibited a sagittal fracture at the screw-bone interface.

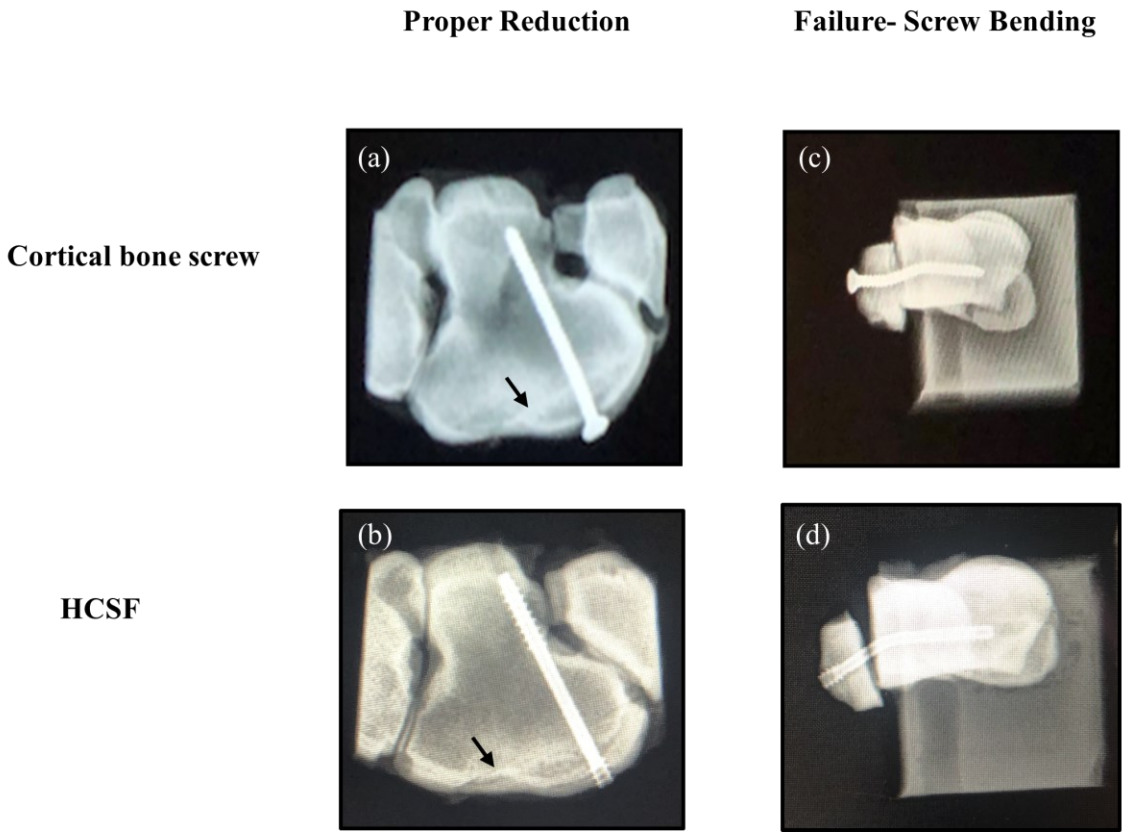

Figure 6 Fragment reduction and common mode of failure

Adequate fragment compression after placement of a cortical bone screw (a) and a HCSF (b). The arrow indicates the fracture plane that has been reduced. Screw bending was observed after testing in all specimens for both the cortical bone screw group as exemplified (c) and HCSF group as exemplified (d).
Credit: Salinger

Table 1 Average maximum load to failure, stiffness, and yield load

	Maximum load to failure (N)	**Stiffness (N/mm)**	**Yield load (N)**
Cortical Screws	2930.19 +/- 707.43	427.59 +/- 128.52	2896.58 +/- 678.57
HCSF Screws	2305.54 +/- 633.44	382.89 +/- 95.27	2291.97 +/- 642.11

Average maximum load to failure, stiffness, and yield load (mean +/- std dev) for simulated C3 frontal plane fractures of the radial facet stabilized with a cortical bone screw or a HCSF.

CHAPTER VI

DISCUSSION

Mechanical testing variables did not differ significantly between screw types. Failure of constructs always began with bending of the screw, and sometimes ended with fracture of the fragment piece (n= 7/18). The force applied by the load cell caused deformation to both the AO cortical screw and HCSF prior to causing fracturing of the bone.

Advantages of the HCSF are its headless design and ability to achieve fragment compression as it is advanced.[58] Complications associated with not countersinking or creating a shallow countersink, such as irritation of dorsal soft tissue structures of the carpus, can potentially be avoided by using the HCSF in place of a cortical bone screw. Applications of this screw for repair of sagittal C3 fractures could be efficacious as the most common complication associated with this type of repair is impingement of the cortical screw head on the second carpal bone.[11] Furthermore, elimination of countersinking with use of the HCSF may enable its application in thin (<10-mm) carpal fragments. The HCSF does not require a glide hole and does not require tapping, which could result in more efficient screw placement. Compression between bone fragments is achieved as the proximal threads of the screw contact the near bone surface. For every revolution of the screwdriver, the fracture is compressed by 0.25 mm, for a maximum of approximately 1.5 mm of compression.[59] This is due to the differing thread pitches from the tip to the head of the screw.

Thoughtful selection of implant material is important due to the vulnerable nature of the radial facet of the third carpal bone. Exercise generally imposes stress to the carpal bones, with the highest area of stress located in the dorsal aspect of the radial facet of the third carpal bone.[21] Materials which have a higher modulus of elasticity are more prone to stress shielding. Stress shielding occurs as a result of an inadequate transfer of stress from an implant to the bone, which impedes the bone's ability to remodel and gain strength.[60] Titanium per ASTM F136 has a modulus of elasticity of 114 GPa, while 316 stainless steel (AO cortical screw implant material) has a higher modulus of elasticity of 186 GPa.[60] With a modulus of elasticity closer to that of bone (approximately 20 GPa in the equine third metacarpus), titanium implants can allow for sufficient load sharing, facilitating callus formation.[61,62] Callus formation leads to remodeling and mineralization, the process by which damaged bone reestablishes its original properties. The cannulated geometry of the HCSF further reduces the global modulus of elasticity. Such osseointegration is theoretically advantageous considering the propensity of this bone to be weaker in relation to surrounding cuboidal bones. Thus, the use of the titanium HCSF may result in more optimal healing in the C3 compared to repairs using 316 stainless steel.

There are possible disadvantages of the HCSF related to its cannulated and headless nature. Cannulated screws are inherently weaker in bending than non-cannulated screws.[60] Lower bending resistance may, however, not be an important design criterion for use in carpal bones, as long bones are more commonly subjected to bending. Additionally, headless screws can be difficult to remove.

The current study did not include ease of insertion of the HCSF compared to the cortical screw as an outcome measure. Initially, the HCSF took longer to place compared to the AO cortical screws; however, by the end of the study the operator was substantially faster at placing

the HCSF screws. Due to the learning curve associated with the use of new implants and instruments, information on the ease of insertion over the course of the study was not recorded.

Several limitations of this study have been recognized. Different equestrian disciplines lead to different mechanical stresses and resultant bone changes.[63] Since cadaveric limbs for this study were collected from horses of different breeds and disciplines, it is presumed that there was some degree of variability in the density of the tested C3 which could have affected biomechanical performance. The ex vivo nature of the study was also unable to account for all (in vivo) factors and forces associated with the fixation and healing of C3 slab fractures, which could pose a limitation in regard to practical application. Nonetheless, the main forces imposed on the carpal bones are those of shear, which has been the focus of this project.[64] Lastly, the sample size was limited, although the number of specimens used for this study is comparable to previous similar investigations.[65,66]

Undoubtedly, the AO cortical screw has been, and remains, the mainstay screw for equine fracture repair. Despite previous investigations of other compression screws, the integration of alternative screw types for simple lag screw fixation have not been widely adopted in equine orthopedics.[65-71] Equine bone is thick and dense, making an AO cortical screw a seemingly obvious choice. The radial facet of the third carpal bone, however, commonly contains relatively increased vascular channels, which reduces its structural integrity and strength.[72] In human orthopedics, osteopenic bone is often unable to withstand the shear forces generated by buttress threaded screws.[73] As a biomechanically inferior area of bone, the same concept may be applicable to the radial facet of the third carpal bone, validating exploration of fracture repair with alternative constructs such as the HCSF. The titanium, interlocking thread

technology of this screw has the potential to improve bone preservation while resisting multiaxial failure.[12]

Maximum load to failure was approximately 2900 N in the cortical screw group and 2300 N in the HCSF group. Reported peak vertical force during stance is approximately 1500 N in horses with an average weight of 430 kg.[74] It is unknown if the constructs tested in this study could withstand forces occurring during a difficult post-operative recovery without additional support. They should, however, have the mechanical integrity to maintain fracture reduction in a horse on stall rest after carpal surgery.

Although a seemingly straightforward orthopedic surgery, C3 slab fracture fixation does not always yield a desirable result. In fact, horses often are unable to perform at their previous level of work despite surgery.[5] It is possible that complications associated with this procedure can be avoided with improved materials and techniques. In the current study, the ability to place the HCSF into the equine C3 has been confirmed, and mechanical performance was not significantly different than the AO cortical screw when tested in shear. If the assumed benefits of the HCSF discussed translate clinically, this implant may lead to better stabilization, faster healing times, and improved animal comfort.

CHAPTER VII

CONCLUSION

Generally speaking, 4.5 or 5.5 mm cortical screws are most commonly used in equine fracture repair and headless screws are very rarely utilized. This begs the question: What applications are there for use of a 3.5 mm screw? Moreover, what applications are there for use of a headless screw?

Cuboidal bone fractures (carpal and tarsal), proximal sesamoid bone fractures, and distal sesamoid fractures often fit criteria for use of 3.5 mm screws. This particularly applies to equids of smaller stature such as ponies and foals. Headless screws are beneficial when placed near important soft tissue structures, bursas, joints, areas that lack sufficient soft tissue coverage, and bones directly covered by tendons or ligaments. When a screw head protrudes from the surface of the bone and makes direct contact with adjacent soft tissues, the friction results in inflammation and can lead to discomfort.

Many carpal and tarsal bone fractures require 3.5 mm screws. As high motion joints, the carpus and tarsus are closely associated with tendons and ligaments that are likely to course directly atop fracture locations. Internal fixation of distal sesamoid bone fractures pose a challenge as this bone is long, narrow, and penetration of the distal interphalangeal joint or navicular bursa can be difficult to avoid.[75] Fractures of the proximal sesamoid bones are common in foals two months of age and younger.[76,77] Foals are ideal candidates for 3.5 mm headless screws due to having structurally smaller, more immature bone. Large apical, midbody,

and basilar proximal sesamoid bone fractures require internal fixation with a lag screw. One or two 2.7 mm, 3.5 mm, or 4.5 mm screws are typically appropriate.[78] The suspensory branches insert proximally on these bones, the distal sesamoidean ligaments originate distally, they communicate with the metacarpophalageal or metatarsophalangeal joint dorsally, and the digital flexor tendon sheath glides across the palmar or plantar aspect of these bones. Screw head interference with any of these structures could cause profound lameness. For these reasons, the discussed fracture types may be repaired with fewer complications applying use of smaller, headless screws.

The results of this study indicate that the HCSF can be successfully placed in the equine third carpal bone. When tested in shear, there was no significant difference in maximum load to failure, stiffness, or yield load when compared to the cortical screws. An overall trend is still recognized as the cortical screws averaged higher maximum loads to failure, stiffness, and yield loads compared to the HCSF screws. It is unknown at this time what trends and levels of significance would be reached with a larger sample size. These results, taken in conjunction with possible benefits of a titanium, headless, interlocking screw, justify a need for clinical validation of the HCSF in further studies, including those investigating use in other anatomical locations.

REFERENCES

1. Secombe CJ, Firth EC, Perkins NR, Anderson BH. Pathophysiology and diagnosis of third carpal bone disease in horses: A review. N Z Vet J 2002; 50:1, 2-8.

2. McIlwraith CW, Yovich JV, Martin GS. Arthroscopic surgery for the treatment of osteochondral chip fractures in the equine carpus. J Am Vet Med Assoc 1987;191:531–40.

3. Graham R, Rosanowski SM, McIlwraith CW. A 10-year study of arthroscopic surgery in racing Thoroughbreds and Quarter Horses with osteochondral fragmentation of the carpus. Equine Vet J 2020;52:225–31.

4. Schneider RK, Bramlage LR, Gabel AA, Barone LM, Kantrowitz BM. Incidence, location and classification of 371 third carpal bone fractures in 313 horses. Equine Vet J 1988;20(Suppl. 6):33–42. 4.

5. Doering AK, Reesink HL, Luedke LK, Moore C, Nixon AJ, Fortier LA, et al. Return to racing after surgical management of third carpal bone slab fractures in thoroughbred and standardbred racehorses. Vet Surg 2019;48:513–23.

6. Nelson BB, Lawless SP, McIlwraith CW. Slab fractures of the third carpal bone involving both radial and intermediate facets and outcomes after surgical repair in racing Quarter Horses. Equine Vet J 2021;00:1–7.

7. Ross MO. Third carpal bone slab fracture repair pathogenesis and decision making. Proceedings from the American College of Veterinary Surgeons Summit. 2012; 67-70.

8. Stephens PR, Richardson DW, Spencer PA. Slab fractures of the third carpal bone in standardbreds and thoroughbreds: 155 cases (1977–1984). J Am Vet Med Assoc 1988;193:353–8.

9. Ruggles AJ. Carpus. In: Auer JA, Stick JA, Kummerle JM, Prange T, editors. Equine Surgery. 5th ed. St. Louis, Missouri: Elsevier; 2019, p. 1655.

10. McIlwraith CW. Diagnostic and Surgical Arthroscopy of the Carpal Joints. In: McIlwraith CW, Nixon AJ, Wright IM, editors. Diagnostic and Surgical Arthroscopy in the Horse. 4th ed. China: Elsevier; 2015, p. 25.

11. Richardson DW. Complications of Orthopaedic Surgery in Horses. Vet Clin North Am Equine Pract 2009;24:591-610.

12. Alfonso NA, Baldini T, and Stahel PF. A New Fastener with Improved Bone-To Implant Interface Shows Superior Torque Stripping Resistance Compared with the Standard Buttress Screw. J Orthop Trauma 2019;33(4):137-142.

13. Stahel PF, Alfonso NA, Henderson C, Baldini T. Introducing the "Bone-Screw-Fastener" for improved screw fixation in orthopedic surgery: a revolutionary paradigm shift? Patient Saf Surg 2017;11:6.

14. DeBaun MR, Swinford ST, Chen MJ, Thio T, Behn AA, Lucas JF, et al. Biomechanical comparison of bone-screw-fasteners versus traditional locked screws in plating female geriatric bone. Injury 2019;14:2.

15. OsteoCentric Technologies, Summit Med Ventures. Our Technology. [accessed 2022 April 11]; 2021. https://www.osteocentric.com/our-technology.

16. Jayesh RS, Dhinakarsamy V. Osseointegraion. J Pharm Bioallied Sci 2015;7(Suppl 1): S226–S229.

17. Engiles JB, Stewart H, Janes J, Kennedy LA. A diagnostic pathologist's guide to carpal disease in racehorses. J of Vet Diag Investigation 2017; 29(4) 414–430.

18. Kaser-Hotz B, Sartoretti-Schefer S, Weiss R. Computed tomography and magnetic resonance imaging of the normal equine carpus. Vet Radiol Ultra 1994:35, 457-461.

19. Gough MR, Mayhew G, Munroe GA. Diffusion of mepivacaine between adjacent synovial structures in the horse. Part 1: forelimb foot and carpus. Equine Vet J 2002;34(1):80-4.

20. Clayton H, Sha D, Stick JA, Mullineaux DR. Three-dimensional carpal kinematics of trotting horses. Equine Vet J 2004;36:671–676.

21. Palmer JL, Bertone AL, Litsky AS. Contact area and pressure distribution changes of the equine third carpal bone during loading. Equine Vet J 1994;26(3):197-202.

22. Cui,W. A state-of-the-art review on fatigue life prediction methods for metal structures. J. Mar Sci Techol 2002;7,43-56.

23. Martig S, Chen W, Lee PVS, Whitton RC. Bone fatigue and its implications for injuries in racehorses. Equine Vet J 2014;46:408-415.

24. Ross MW, Richardson DW, Beroza GA. Subchondral lucency of the third carpal bone in Standardbred racehorses: 13 cases (1982-1988). J Am Vet Med Assoc 1989;195(6):789-94.

25. Kawcak CE, McIlwraith CW, Norrdin RW, Park RD and Steyn PS. Clinical effects of exercise on subchondral bone of carpal and metacarpophalangeal joints in horses. Am J Vet Res 2000;61:1252-1258.

26. Uhlhorn H, Carlsten J. Retrospective study of subchondral sclerosis and lucency in the third carpal bone of Standardbred trotters. Equine Vet J 1999;31:500–505.

27. Riggs CM. Fractures – a preventable hazard of racing Thoroughbreds? Vet J 2002;163: 19-29.

28. Markel MD. Bone Structure and the Response of Bone to Stress. In: Nixon AJ, editor. Equine Fracture Repair. 2nd ed. Elmont, NY: Wiley Blackwell; 2020, p. 3-11.

29. Chamay A and Tschantz P. Mechanical influences in bone remodeling. Experimental research on Wolff's law. J Biomech 1972;5: 173–180.

30. Dempster WT and Coleman, R.F. Tensile strength of bone along and across the grain. J Appl Physiol 1960;16: 355.

31. Lanyon LE. Mechanical function and bone remodeling. In: Sumner-Smith G, editor. Bone in Clinical Orthopedics. Philadelphia: WB Saunders Co; 1982, p. 273-304.

32. Nunamaker DM, Butterweck DM, Provost MT. Some geometric properties of the third metacarpal bone: a comparison between the Thoroughbred and Standardbred racehorse. J Biomech 1989;22:129–134.

33. Radin EL, Orr RB, Kelman JL. et al. Effect of prolonged walking on concrete on the knees of sheep. J Biomech 1982;15:487–492.

34. Rubin CT and Lanyon LE. Osteoregulatory nature of mechanical stimuli: function as a determinant for adaptive remodeling in bone. J Orthop Res 1987;5: 300–310.

35. Woo SLY, Kuei SC, Amiel D, et al. The effect of prolonged physical training on the properties of long bone: a study of Wolff's law. J Bone Joint Surg Am 1981;63:780–787.

36. Tidswell HK, Innes JF, Avery NC, Clegg PD, Barr ARS, Vaughan-Thomas A, Wakley G, Tarlton JF. High-intensity exercise induces structural, compositional, and metabolic changes in cuboidal bones- findings from an equine athlete model. Bone 2003;43:724-733.

37. Hayes WC and Snyder B. Toward a quantitative formulation of Wolff's law in trabecular bone. In: Cowin SC, editor. Mechanical Properties of Bone. AMD. New York: American Society of Mechanical Engineers; 1981, 45:43-68.

38. Lopez MJ. Bone Biology and Fracture Healing. In: Auer JA, Stick JA, Kummerle JM, Prange T, editors. Equine Surgery. 5th ed. St. Louis, MO: Elsevier; 2019, p. 1255-1268.

39. Markel MD. Bone Structure and the Response of Bone to Stress. In: Nixon AJ, editor. Equine Fracture Repair. 2nd ed. Elmont, NY: Wiley Blackwell; 2020, p. 12-23.

40. Bramlage LR, Schneider RK, Gabel AA. A Clinical perspective on lameness originating in the carpus. Eq Vet J 1988;20(6):12-18.

41. Kaderly RE. Primary bone healing. Semin Vet Med Surg (Small Anim) 1991;6(1):21–25.

42. Hulse D, Hyman B. Fracture Biology and Biomechanics. In: Slatter D, editor. Textbook of small animal surgery. WB Saunders; Philadelphia: 1993. pp. 1595–1603.

43. Schenk RK, Hunziker EB. Histologic and ultrastructural features of fracture healing. In: Brighton CT, Friedlander GE, Lane JM, editors. Bone formation and repair. American Academy of Orthopedic Surgeons; Rosemont: 1994. pp. 117–145.

44. Marsell R, Einhorn TA. The Biology of Fracture Healing. Injury 2011;42(6): 551–555.

45. Cho TJ, Gerstenfeld LC, Einhorn TA. Differential temporal expression of members of the transforming growth factor beta superfamily during murine fracture healing. *Journal of Bone & Mineral Research.* 2002;17(3):513–20.

46. Einhorn TA. The cell and molecular biology of fracture healing. Clinical Orthopaedics & Related Research. 1998;355(Suppl):S7–21.

47. Wendeberg B. Mineral metabolism of fractures of the tibia in man studied with external counting of Sr85. Acta Orthopaedica 1961;52:1–79.

48. Shefelbine SJ, Augat P, Claes L, Simon U. Trabecular bone fracture healing simulation with finite element analysis and fuzzy logic. Journal of Biomechanics 2005;38(12):2440-2450.

49. Calinger R, Brown JE, West TR. Ancient mathematical zenith in the hellenistic third century B.C., II: Archimedes to Diocles. Calinger RS. ed. A Contextual History of Mathematics: To Euler. Upper Saddle River, NJ: Prentice Hall, 1999; 150-169.

50. Robers TT, Prummer CM, Papaliodis DN, Uhl RL, Wagner TA. History of the Orthopedic Screw. Orthopedics 2013;(36)1:12-14.

51. Klenerman L. *The Evolution of Orthopaedic Surgery.* London, United Kingdom: The Royal Society of Medicine; 2002.

52. Sauerbier S, Schön R, Otten JE, Schmelzeisen R, Gutwald R. The development of plate osteosynthesis for the treatment of fractures of the mandibular body - a literature review. J Craniomaxillofac Surg 2008;36(5):251-9.

53. Matter P. History of the AO and its global effect on operative fracture treatment. Clin Orthop Relat Res 1998;(347):11-8.

54. Raleigh JS, Filliquist B, Kapatkin AS, Chou PY, Marcellin-Little DJ, Farcia TC, Stover SM. Influence of interlocking thread screws to repair simulated adult canine humeral condylar fractures. Vet Surg 2021;50(6):1237-1249.

55. Kenzig AR, Butler JR, Priddy LB, Lacy KR, Elder SH. A biomechanical comparison of conventional dynamic compression plates and string-of-pearls™ locking plates using cantilever bending in a canine Ilial fracture model. BMC Vet Res 2017;13:222.

56. Whitney ME, Butler JR, Dycus DL, Teer TB, Elder SH, Priddy LB, et al. Ex vivo biomechanical comparison of four Center of Rotation Angulation Based Leveling Osteotomy fixation methods. Vet Surg 2002;51(1):157-162.

57. Blakely JA, Butler JR, Priddy LB, McCabe EM, Avendano JN, Elder SH, et al. Ex vivo biomechanical comparison of 2.7 mm string-of-pearl plate versus screw/wire/Polymethylmethacrylate composite fixation and 2.7 mm veterinary acetabular plate for repair of simulated canine acetabular fractures. BMC Vet Res 2019;15:287.

58. OsteoCentric Technologies, Summit Med Ventures. Current Products. [accessed 2022 April 11]; 2021. https://www.osteocentric.com/headless-compression-system.

59. OsteoCentric Technologies, Summit Med Ventures. Surgical Technique. [accessed 2022 April 11]; 2021. https://www.osteocentric.com/_files/ugd/709b71_c98156cdcb604b0998b31009b2f314d0.pdf.

60. Auer JA. Principles of Fracture Treatment. In: Auer JA, Stick JA, Kummerle JM, Prange T, editors. Equine Surgery. 5th ed. St. Louis, Missouri: Elsevier; 2019, p. 1288-1289.

61. Gibson VA, Stover SM, Giveling JC, Hazelwood SJ, Martin RB. Osteonal effects of elastic modulus and fatigue life in the equine bone. J Biomech 2006;9(2):217-225.

62. Tapscott DC, Wottowa C. Orthopedic Implant Materials. [Updated 2021 Jul 31]. In: StatPearls [Internet]. Treasure Island (FL): StatPearls Publishing; 2022 Jan. Available from: https://www.ncbi.nlm.nih.gov/books/NBK560505/.

63. Firth EC, Delahunt J, Wichtel JW, Birch HL and Goodship AE. Galloping exercise induces regional changes in bone density within the third and radial carpal bones of Thoroughbred horses. Equine Vet J 1999;31:111-115.

64. Bramlage LR, Schneider RK, Gabel AA: A clinical perspective on lameness originating in the carpus. Equine Vet J Suppl 1998;6:12-18.

65. Murray RC, Gaughan EM, Debowes RM, Hoskinson JJ. Biomechanical Comparison of the Herbert and AO Cortical Bone Screws for Compression of an Equine Third Carpal Bone Dorsal Plane Slab Osteotomy. Vet Surg1998;27:49–55.

66. Bueno ACD, Galuppo LD, Taylor KT, Jensen DG, Stover SM. A bio-mechanical comparison of headless tapered variable pitch and AO cortical bone screws for fixation of a simulated slab fracture in equine third carpal bones.Vet Surg 2003;32(2):167-177.

67. Eddy AL, Galuppo LD, Stover SM, Taylor KT, Jensen DG. A Biomechanical Comparison of Headless Tapered Variable Pitch Compression and AO Cortical Bone Screws for Fixation of a Simulated Midbody Transverse Fracture of the Proximal Sesamoid Bone in Horses. Vet Surg 2004;33:253-262.

68. Herthel DJ, Moody JL, Lauper I. The repair of condylar fractures of the third metacarpal bone and the third metatarsal bone using the Herbert compression screw in nine Thoroughbred racehorses. Equine Pract 1995;19:6-12.

69. Galuppo LD, Stover SM, Jensen DG, Willits NH. A biomechanical comparison of headless tapered variable pitch and AO cortical bone screws for fixation of simulated lateral condylar fractures in equine third metacarpal bones. Vet Surg 2001;30:332-340.

70. Galuppo LD, Stover SM, Jensen DG. A biomechanical comparison of equine third metacarpal condylar bone fragment compression and screw pushout strength between headless tapered variable pitch and AO cortical bone screws. Vet Surg 2002;31:201-210.

71. Lewis AJ, Sod GA, Burba DJ, Mitchell CF. Compressive forces achieved in simulated equine third metacarpal bone lateral condylar fractures of varying fragment thickness with Acutrack Plus screws and 4.5 mm AO cortical screws. Vet Surg 2010;39:78-82.

72. Kim W, McArdle BH, Kawcak CE, McIlwraith CW, Firth EC, Broom ND. Histomorphometric evaluation of the effect of early exercise on subchondral vascularity in the third carpal bone of horses. Am J Vet Res 2013;74(4), 542-549.

73. Egol KA, Kubiak EN, Fulkerson E, Kummer FJ, Koval KJ. Biomechanics of locked plates and screws. J Orthop Trauma 2004;18:488-93.

74. Kingsburg HB, Quddus MA, Rooney JR, Geary JE. A laboratory system for production of flexion rates and forces in the forelimb of the horse. Am J Vet Res 1978;39(3):365-9.

75. Schramme MC. Fractures of the Navicular Bone. In: Nixon AJ, editor. Equine Fracture Repair. 2nd ed. Elmont, NY: Wiley Blackwell; 2020, p. 242-255.

76. Ellis DR. Fractures of the proximal sesamoid bones in thoroughbred foals. Equine Vet J 1979;11:48–52.

77. Reesink HL. Foal fractures: osteochondral fragmentation, proximal sesamoid bone fractures/ sesamoiditis, and distal phalanx fractures. Vet Clin North Am Equine Pract 2017;33:397–416.

78. Wright IM. Fractures of the Proximal Sesamoid Bones. In: Nixon AJ, editor. Equine Fracture Repair. 2nd ed. Elmont, NY: Wiley Blackwell; 2020, p. 341-373.

APPENDIX A

RAW DATA INDIVIDUAL SPECIMENS

Table 2 Stiffness, maximum load to failure, and yield load for individual specimens

Sample Label	Stiffness (N/mm)	Max Load (N)	Yield Load (N)
3LF	549.96	3146.97	3134.407
3RC	543.04	1458.07	
4LC	486.73	3275.18	3157.5195
4RF	399.34	2971.83	
6LC	273.6	2853.26	
6RF	244.9	1352.76	1308.0742
7LF	387.18	2116.8	2073.3252
7RC	271.39	2811.06	
8LC	346.04	2643.05	
8RF	300.87	2135.7	
9LF	386.66	2458.58	2443.051
9RC	490.02	3724.85	
10LC	590.01	3913.05	3772.9524
10RF	317.14	1449.22	1443.3173
11LF	359.69	2875.68	2875.677
11RC	300.8	2804.90	2760.137
12LC	546.71	2888.31	
12RF	500.24	2242.35	

Sample label refers to the carpal specimen used. The number is the horse identity, L or R signifies left (L) or right (R) limb used, and F or C represents repair with the headless compression screw fastener (F) or cortical screw (C). Yield load was calculated using a 1 mm offset.

APPENDIX B

RAW DATA OVERALL SUMMARY

Table 3 Overall Results- All Specimens

ALL SPECIMENS	
Average Max Load	2617.868 N
Standard Deviation Max Load	+/- 726.3716 N
Average Stiffness	405.24 N/mm
Standard Deviation Stiffness	+/- 112.1295N/mm
Average Yield Load	2594.27 N
Standard Deviation Yield Load	+/- 712.3695 N

Maximum load, stiffness, and yield load averages calculated for all specimens in both groups.

Table 4 Overall Results- HCSF Group

HCSF GROUP	
Average Max Load	2305.54 N
Standard Deviation Max Load	+/- 633.439 N
Average Stiffness	382.8867 N/mm
Standard Deviation Stiffness	+/- 95.27359 N/mm
Average Yield Load	2291.97 N
Standard Deviation Yield Load	+/- 642.1059 N

Maximum load, stiffness, and yield load averages calculated for all specimens in the HCSF group.

Table 5 Overall Results- Cortical Screw Group

CORTICAL GROUP	
Average Max Load	2930.19 N
Standard Deviation Max Load	+/- 707.4306 N
Average Stiffness	427.5933 N/mm
Standard Deviation Stiffness	+/- 128.5161 N/mm
Average Yield Load	2606.92 N
Standard Deviation Yield Load	+/- 678.5659 N

Maximum load, stiffness, and yield load averages calculated for all specimens in the cortical screw group.

.